

Article

How Do Small Differences in Geometries Affect Electrostatic Potentials of High-Energy Molecules? Critical News from Critical Points

Danijela S. Kretić, Vesna B. Medaković and Dušan Ž. Veljković * 

University of Belgrade–Faculty of Chemistry, Studentski trg 12-16, 11000 Belgrade, Serbia

* Correspondence: vdusan@chem.bg.ac.rs

Abstract: The computational design of explosives is becoming very popular since it represents a safe and environmentally friendly way of predicting the properties of these molecules. It is known that positive values of electrostatic potential in the central areas of the molecular surface are a good indicator of the sensitivity of high-energy materials towards detonation. The molecular electrostatic potential is routinely calculated for molecules of explosives using both geometries extracted from crystal structures, and computationally optimized geometries. Here we calculated and compared values of positive electrostatic potential in the centers of five classical high-energy molecules for geometries extracted from different crystal structures and theoretically optimized geometries. Density functional theory calculations performed at M06/cc-PVDZ level showed that there are significant differences in the values of electrostatic potentials in critical points obtained for different geometries of the same high-energy molecules. The study also showed that there was an excellent agreement in the values of electrostatic potentials calculated for optimized geometry of 1,3,5-trinitrobenzene and geometry of this molecule obtained by neutron diffraction experiments. The results of this study could help researchers in the area of the computational development of high-energy molecules to better design their studies and to avoid the production of erroneous results.

Keywords: high-energy materials; crystal structure; molecular electrostatic potential; density functional theory



Citation: Kretić, D.S.; Medaković, V.B.; Veljković, D.Ž. How Do Small Differences in Geometries Affect Electrostatic Potentials of High-Energy Molecules? Critical News from Critical Points. *Crystals* **2022**, *12*, 1455. <https://doi.org/10.3390/cryst12101455>

Academic Editor: Thomas M. Klapötke

Received: 17 September 2022

Accepted: 9 October 2022

Published: 14 October 2022

Publisher's Note: MDPI stays neutral with regard to jurisdictional claims in published maps and institutional affiliations.



Copyright: © 2022 by the authors. Licensee MDPI, Basel, Switzerland. This article is an open access article distributed under the terms and conditions of the Creative Commons Attribution (CC BY) license (<https://creativecommons.org/licenses/by/4.0/>).

1. Introduction

The development of new classes of high-energy materials (HEM) with improved detonation performance and moderate sensitivity towards detonation is the ultimate goal of many theoretical and experimental studies [1–6]. Properties of new HEM compounds could be predicted by analysis of crystalline and molecular factors that play role in the initiation of the detonation process [7]. Crystalline factors strongly affect both efficiency and sensitivity toward detonation of high-energy materials in the solid state [2,4]. Crystal properties that have the most important roles in defining the detonation characteristics of HEM molecules are crystal density and free space per molecule in the crystal lattice [2]. It is known that high crystal density promotes better detonation performance of HEM molecules [2]. It is also known that a small amount of free space in crystal lattice lowers the sensitivity of high-energy materials towards detonation [2,4]. For these reasons, analysis of crystal structures of HEM molecules is a crucial step in the assessment of different detonation characteristics of explosives, from detonation velocity to impact sensitivity [1,8]. On the other hand, molecular properties like energy content, oxygen balance, molecular electrostatic potential, bond dissociation energies, atomic charges, and many others are also identified as factors that affect the sensitivity of explosives toward detonation [8,9]. One of the most important tools in the assessment of the impact sensitivities of HEM molecules is Molecular Electrostatic Potential (MEP). Numerous studies showed that there is a link between positive values of the electrostatic potentials above the central regions of the

molecular surface and sensitivity toward detonation of certain classes of explosives [10–12]. For nitroaromatic explosives, values of positive potential at the critical points (CPs) located above the aromatic rings could be used to assess trends in sensitivity toward detonation. Critical points represent the most electron-rich (V_{\min}) or electron-depleted (V_{\max}) sites of the molecular electrostatic potential [13]. It is important to point out that molecular electrostatic potential is the physical characteristic of a molecule which could be both experimentally determined and calculated by ab initio calculations. However, due to the constant demands for safer and environmentally-friendly procedures for the design and production of highly energetic molecules, computational simulations are becoming a widely-accepted tool for the prediction of different characteristics of explosives, especially molecular electrostatic potential [2,4,7,8]. In practice, the calculation of MEP can be done using both geometries from crystal structures and computationally optimized geometries [14–17]. In our recent studies, we used both computationally optimized geometries and geometries of HEM molecules extracted from crystal structures to predict the effect of hydrogen and halogen bonding on the modification of electrostatic potentials of nitroaromatic explosives [16,17]. In these studies, geometries from crystal structures were used to study the influence of the surrounding molecules in crystal structures on the electrostatic potentials of nitroaromatic molecules. Depending on the methodology used to optimize geometry in quantum chemical calculations, the quality of crystal samples and methodology used to determine the position of atoms in crystal structures, differences in geometries (atomic distances and angles) between computationally and experimentally determined geometries of HEM molecules could be noticed [18]. Also, there are differences in the geometries in crystal structures of the same molecules which were crystallized under different conditions.

In this work, we quantitatively studied how these differences in geometries affect values of calculated electrostatic potentials in critical points of selected nitroaromatic explosives. A recent study of charge distribution in crystals of organic explosives showed that MEP values and sensitivity toward detonation of selected nitroaromatic and nitroaliphatic explosives are strongly affected by the changes in the geometry of nitro-groups in these molecules [19]. Also, an experimental study of charge relocations in aspirin molecule showed that discrete motions of methyl group result in significant changes in charge distribution in the aromatic system of aspirin [20]. Analysis of electrostatic potential values and sensitivity towards detonation of TNT and CL20 (Hexanitrohexaazaisowurtzitane) molecules in CL20/TNT co-crystals represent a good example of the importance of variation of electrostatic potential values on the properties of highly energetic molecules [21]. The CL20/TNT adducts is less sensitive towards detonation compared to CL-20 but more sensitive compared to TNT molecule. Computational study performed on this adduct and analysis of the calculated electrostatic potential maps showed that in the CL-20/TNT co-crystal positive electrostatic potential on the molecular surface of CL-20 molecule is weaker in comparison to the values of positive electrostatic potential of free molecules. Analysis of the electrostatic potential on the molecular surface of the TNT molecule in CL20/TNT adducts showed that positive potential on the surface of the TNT molecule is stronger in comparison to positive potential values on the surface of free TNT molecule. This analysis clearly indicates the importance of the variations in electrostatic potential values on the properties of high-energy molecules.

To study the influence of small differences in geometries on electrostatic potential values, we calculated MEPs for different crystal structures of the same HEM molecules (obtained under different conditions or from samples of different quality) and compared positive values of the electrostatic potential in critical points for all studied molecules. We also compared the values of positive electrostatic potentials above the central regions of molecular surfaces computed on geometries extracted from crystal structures with the values of electrostatic potentials computed on computationally optimized geometries of studied HEM molecules.

In addition, the influence of the small differences in geometries on energy and geometry of C-H/O interactions involving HEM molecules as hydrogen atom donors was

analyzed. It is known that the presence of C-H/O interactions involving nitroaromatic C-H donors may contribute to the modification of electrostatic potential values [16].

Based on these results, suggestions for the selection of the starting geometries for the electrostatic potential maps were formulated with the respect to the particular demands in the field of the design of high-energy materials.

2. Materials and Methods

Cambridge Structural Database (CSD) was searched for all crystal structures containing molecules of five well-known nitroaromatic explosives: 1,3,5-Trinitrobenzene (TNB), 2,4,6-Trinitrophenol (TNP), 2,4,6-Trinitrotoluene (TNT), TATB (2,4,6-triamino-1,3,5-trinitrobenzene) and the TETRYL (2,4,6-Trinitrophenylmethylnitramine) [22]. Three-dimensional structures of these molecules are given in Figure 1. Only non-disordered, non-polymeric crystal structures without errors and with an R factor ≤ 0.1 were analyzed in the frame of this study. Among extracted structures, those that contained other molecules or co-crystals of studied HEM molecules were not considered for further analysis. Lists of refcodes of all extracted structures are given in Tables S1–S3 in the Supplementary Material. Crystal structure TNBENZ10 was separately analyzed since it was obtained by a very precise neutron diffraction experiment. Since the neutron diffraction structure was available only for TNB molecule, electrostatic potential maps calculated for the structures obtained by X-ray experiments were compared to the electrostatic potential maps calculated for the structures obtained by neutron diffraction experiment and theoretically optimized geometries. The values of the positive potential in the center of aromatic ring were very similar for theoretically optimized geometry of the TNB and geometry obtained by neutron diffraction, and for that reason for all the other molecules of the explosives electrostatic potentials calculated for geometries extracted from crystal structures were compared to the electrostatic potentials calculated for the theoretically optimized geometry. Wave function files needed for the MEP calculations were obtained using the Gaussian09 software package [23]. Based on the calculated wave function files, electrostatic potential maps were calculated and visualized using Wave Function Analysis—Surface Analysis Suite (WFA-SAS) software [24]. Electrostatic potential maps were calculated at the M06/cc-pVDZ level of theory since this level of theory was successfully used for similar calculations in previous studies [16,25]. Critical points in electrostatic potential maps, and not in electron density were considered for the analysis. The energy of C-H/O interactions was calculated using the MP2 method and cc-pVTZ basis set since this level of theory was previously proved to give excellent results for C-H/O interactions involving aromatic C-H donors and oxygen atoms from water molecules [26]. Three-dimensional structures were visualized using Mercury software [27]. The IR frequencies were calculated for all optimized geometries and analysis showed that the equilibrium state has been reached (Figures S1–S5.)

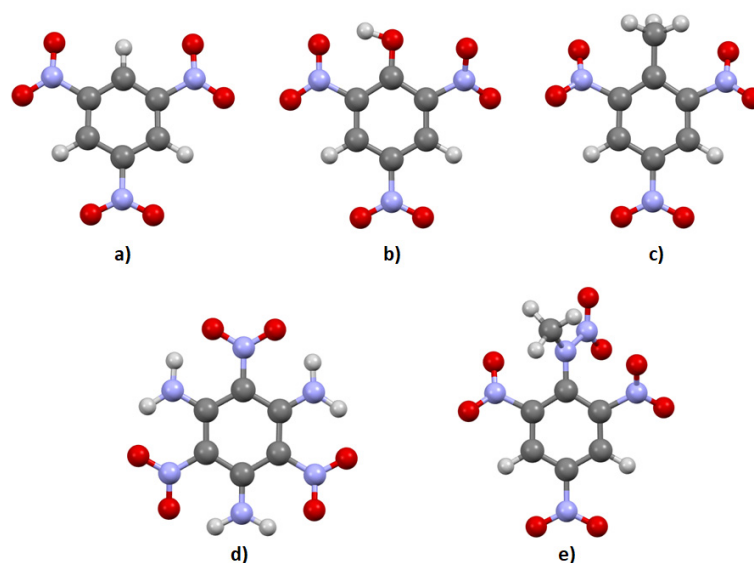


Figure 1. Optimized geometries of (a) 1,3,5-Trinitrobenzene (TNB), (b) 2,4,6-Trinitrophenol (TNP), and (c) 2,4,6-Trinitrotoluene (TNT), (d) 2,4,6-Triamino-1,3,5-trinitrobenzene (TATB) and (e) 2,4,6-Trinitrophenylmethylnitramine (TETRYL).

3. Results

3.1. Molecular Electrostatic Potential Calculations

Electrostatic potential maps were calculated on geometries of TNB, TNP, and TNT crystal structures extracted from the Cambridge Structural Database. CSD was searched for all crystal structures that contain molecules of TNB, TNP, and TNT. Results showed that there were 92 crystal structures containing TNB molecule, 61 structures containing TNP molecule, and 29 structures containing TNT molecule archived in CSD. However, since in many of these structures, nitroaromatic molecules were co-crystallized with other molecules and since it is known that co-crystallization may affect electrostatic potential values, only those structures without any additional molecules were used for electrostatic potential map calculations.

Calculated electrostatic potential maps for crystal structures containing TNB molecule (refcodes: TNBENZ10, TNBENZ11, TNBENZ12, TNBENZ13, and TNBENZ14) are given in Figure 2. It is important to note that TNBENZ10 crystal structure was obtained by neutron diffraction experiment, while all the other crystal structures were determined by X-ray diffraction experiments.

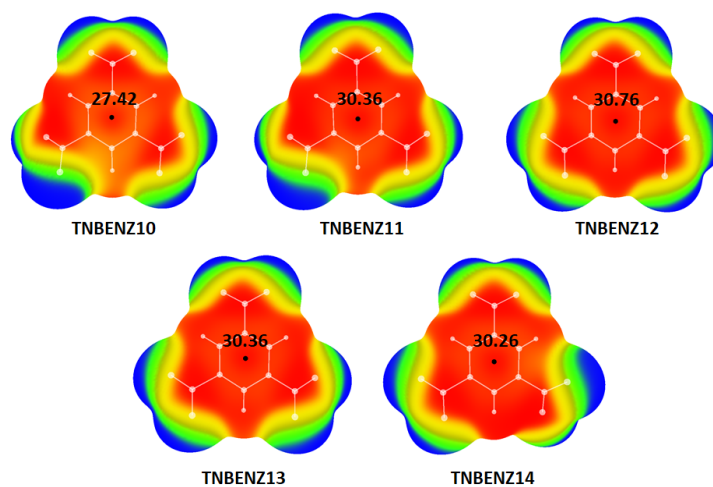


Figure 2. Electrostatic potential maps calculated for the geometries of TNT molecule found in crystal structures archived in CSD. Color ranges (in kcal/mol): red, greater than 20.92, yellow, from 0.00 to 20.92, green, from -6.99 to 0.00, and blue, more negative than 6.99.

Calculated values of positive electrostatic potential above the central area of molecular surfaces are: 27.42 kcal/mol for TNBENZ10; 30.36 kcal/mol for TNBENZ11; 30.76 kcal/mol for TNBENZ12; 30.36 kcal/mol for TNBENZ13 and 30.26 kcal/mol for TNBENZ14. These values were compared to previously calculated values of electrostatic potential for computationally optimized geometry of TNB molecule (Table 1) [16].

Table 1. Total energies, V_{\max} deviations, and V_{\max} values in critical points above the centers of nitroaromatic rings calculated for selected crystal structures containing TNB molecule.

Structure	V_{\max} ¹ (kcal/mol)	E (Hartree)	V_{\max} Deviation ² (%)
TNBENZ10	27.42	−845.3461488	0.35
TNBENZ11	30.36	−845.3002792	11.08
TNBENZ12	30.76	−845.2847208	12.56
TNBENZ13	30.36	−845.3030868	11.10
TNBENZ14	30.26	−845.3006406	10.72
Optimized TNB ³	27.33	−845.35482453	/

¹ Value of positive potential in the critical point located above the central area of the aromatic ring. ² Deviation from V_{\max} value calculated for the critical point in the optimized structure. ³ Electrostatic potential value taken from ref. [16].

Results of the electrostatic potential calculations indicated that there are significant differences in the values of positive potential between different three-dimensional structures of the TNB molecule, as well as between computationally optimized and experimentally determined geometries of this molecule. The most significant deviation compared to computationally optimized geometry was calculated for the TNBENZ12 structure (12.56% deviation from the electrostatic potential value of computationally optimized TNB molecule). However, the results of the analysis showed that the calculated value of the positive electrostatic potential in the selected critical point for computationally optimized TNB structure was in good agreement with the value calculated for the TNBENZ10 structure. This is not unexpected since the TNBENZ10 structure was determined using a very accurate neutron diffraction technique. Analysis of the calculated total energies of selected structures showed that the total energy of the TNBENZ10 structure was the lowest compared to the other crystal structures (−845.3461488 Hartree).

Similar analyses of electrostatic potential maps were performed for the other two nitroaromatic molecules, TNP and TNT. Calculated electrostatic potential maps for the crystal structures of the TNP molecule are given in Figure 3.

In the case of the TNP, large deviations in the calculated values of the electrostatic potential in critical points occurred between optimized structure and crystal structures. Calculated deviations in the values of the positive potential in the central regions of molecular surface for geometries of the TNP extracted from crystal structures are given in Table 2.

The most significant deviation was calculated for the PICRAC11 structure in which electrostatic potential in the critical point above the center of the molecule was calculated to be 32.82 kcal/mol (19.40% deviation from the electrostatic potential value of computationally optimized TNP molecule) [16]. The smallest deviation in the values of critical points compared to the optimized structure was calculated for the PICRAC structure (V_{\max} = 29.57 kcal/mol which represents a 7.56% deviation from the electrostatic potential value of the computationally optimized TNB molecule).

Large deviations from electrostatic potential values calculated for optimized geometry were also found for all the other geometries extracted from crystal structures: PICRAC19 (16.31%), PICRAC18 (15.78%), PICRAC13 (15.62%), PICRAC17 (15.48%), PICRAC15 (14.82%), PICRAC16 (14.27%) and PICRAC14 (13.86%).

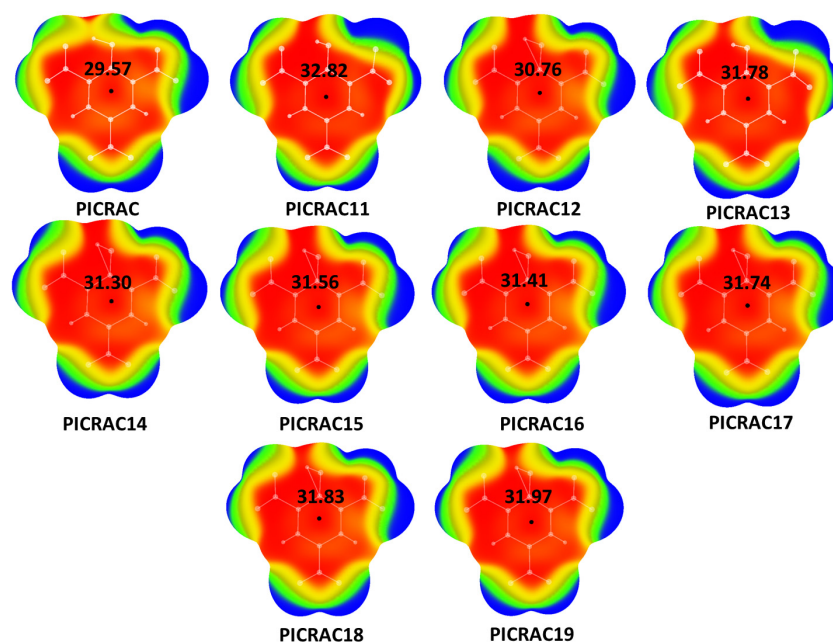


Figure 3. Electrostatic potential maps calculated for the geometries of TNP molecule (picric acid) found in crystal structures archived in CSD. Color ranges (in kcal/mol): red, greater than 20.92, yellow, from 0.00 to 20.92, green, from -6.99 to 0.00, and blue, more negative than 6.99.

Table 2. Total energies, V_{\max} deviations, and V_{\max} values in critical points above the centers of nitroaromatic rings calculated for selected crystal structures containing TNP molecule.

Structure	V_{\max} ¹ (kcal/mol)	E (kcal/mol)	V_{\max} Deviation ² (%)
PICRAC	29.57	−920.4130444	7.56
PICRAC11	32.82	−920.2254342	19.40
PICRAC12	31.51	−920.5205850	14.64
PICRAC13	31.78	−920.4575628	15.62
PICRAC14	31.30	−920.4979973	13.86
PICRAC15	31.56	−920.4979960	14.82
PICRAC16	31.41	−920.4980897	14.27
PICRAC17	31.74	−920.4872273	15.48
PICRAC18	31.83	−920.4745691	15.78
PICRAC19	31.97	−920.4732924	16.31
Optimized TNP ³	27.49	−920.55863946	/

¹ Value of positive potential in the critical point located above the central area of the aromatic ring. ² Deviation from V_{\max} value calculated for the critical point in the optimized structure. ³ Electrostatic potential value taken from ref. [16].

Large deviations in the electrostatic potential values in studied critical points were observed between crystal structures containing TNT molecule (Figure 4). However, there was no deviation between V_{\max} values calculated for ZZZMUC06 crystal structure and computationally optimized geometry of TNT. Calculated deviations in the values of the positive potential in the central regions of molecular surface for geometries of TNT molecule extracted from crystal structures are given in the Table 3.

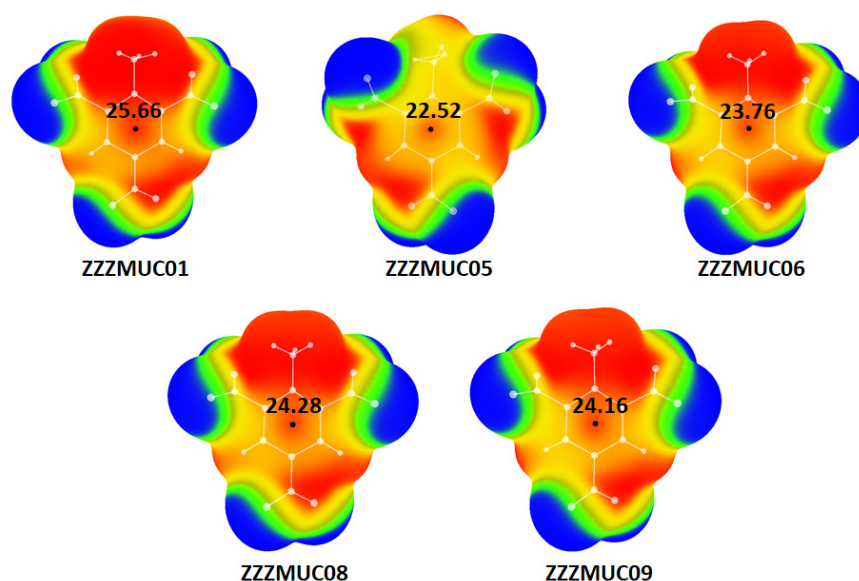


Figure 4. Electrostatic potential maps calculated for the geometries of TNT molecule found in crystal structures achieved in CSD. Color ranges (in kcal/mol): red, greater than 20.92, yellow, from 0.00 to 20.92, green, from -6.99 to 0.00, and blue, more negative than 6.99.

Table 3. Total energies, V_{\max} deviations and V_{\max} values in critical points above the centers of nitroaromatic rings calculated for selected crystal structures containing TNT molecule.

Structure	V_{\max} ¹ (kcal/mol)	E (kcal/mol)	V_{\max} Deviation ² (%)
ZZZMUC01	25.66	-884.49156794	7.98
ZZZMUC05	22.52	-884.489125884	5.20
ZZZMUC06	23.76	-884.557859799	0.00
ZZZMUC08	24.28	-884.554014599	2.19
ZZZMUC09	24.16	-884.562118641	1.70
Optimized TNT ³	23.76	-884.581835322	/

¹ Value of positive potential in the critical point located above the central area of the aromatic ring. ² Deviation from V_{\max} value calculated for the critical point in the optimized structure. ³ Electrostatic potential value taken from ref. [16].

V_{\max} values calculated for geometries extracted from selected crystal structures (Figure 4) were in the range of 22.52–25.66 kcal/mol. Generally, this is in good agreement with the V_{\max} value obtained for the computationally optimized geometry of TNT (23.76 kcal/mol) [16]. Only in cases of ZZZMUC01 and ZZZMUC05 relatively large deviations were observed (7.98% and 5.20%, respectively).

Significant deviations in the values of positive electrostatic potential were also observed between crystal structures containing TATB molecule (Figure 5).

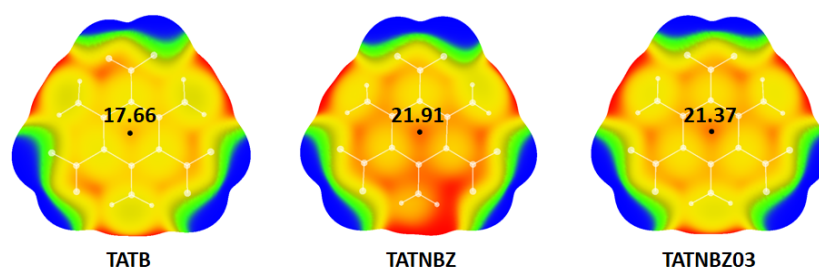


Figure 5. Electrostatic potential maps calculated for the optimized geometry (TATB) and geometries of TATB molecule found in crystal structures achieved in CSD (TATNBZ and TATNBZ03). Color ranges (in kcal/mol): red, greater than 20.90, yellow, from 0.00 to 20.90, green, from -6.99 to 0.00, and blue, more negative than 6.99.

The V_{\max} values calculated for geometries extracted from selected crystal structures (Figure 5) were 21.91 kcal/mol for TATNBZ crystal structure and -21.37 kcal/mol for TATNBZ03 structure. For both structures there was a significant difference in the electrostatic potential value compared to the computationally optimized geometry of TATB molecule (17.66 kcal/mol). Calculated deviations are given in Table 4.

Table 4. Total energies, V_{\max} deviations and V_{\max} values in critical points above the centers of nitroaromatic rings calculated for selected crystal structures containing TNT molecule.

Scheme 1.	V_{\max} ¹ (kcal/mol)	E (kcal/mol)	V_{\max} Deviation ² (%)
TATNBZ	25.66	-1011.1872097	21.01
TATNBZ03	22.52	-1011.3807914	24.07
Optimized TATB	23.76	-1011.3867634	

¹ Value of positive potential in the critical point located above the central area of the aromatic ring. ² Deviation from V_{\max} value calculated for the critical point in the optimized structure.

Electrostatic potential maps calculated for the optimized TETRYL geometry and TETRYL geometries extracted from the crystal structures are given in the Figure 6.

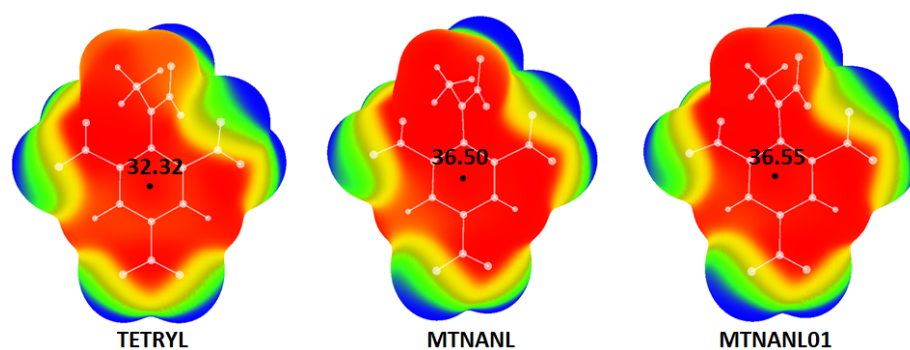


Figure 6. Electrostatic potential maps calculated for the optimized geometry (TETRYL) and geometries of TETRYL molecule found in crystal structures achieved in CSD (MTNANL and MTNANL01). Color ranges (in kcal/mol): red, greater than 20.90, yellow, from 0.00 to 20.90, green, from -6.99 to 0.00, and blue, more negative than 6.99.

The V_{\max} values calculated for geometries extracted from selected crystal structures (Figure 6) were 36.50 kcal/mol for MTNANL crystal structure and -36.55 kcal/mol for MTNANL01 structure. For both structures there was a significant difference in the electrostatic potential value compared to the computationally optimized geometry of TETRYL molecule (32.32 kcal/mol). Calculated deviations are given in Table 5.

Table 5. Total energies, V_{\max} deviations and V_{\max} values in critical points above the centers of nitroaromatic rings calculated for selected crystal structures containing TNT molecule.

Structure	V_{\max} ¹ (kcal/mol)	E (kcal/mol)	V_{\max} Deviation ² (%)
MTNANL	36.50	-1144.2011083	12.93
MTNANL01	36.55	-1144.2184993	13.09
Optimized TETRYL	32.32	-1144.3552437	

¹ Value of positive potential in the critical point located above the central area of the aromatic ring. ² Deviation from V_{\max} value calculated for the critical point in the optimized structure.

3.2. Interaction Energies Calculations

Since many noncovalent interactions like hydrogen bonds are electrostatic in nature, it was reasonable to expect that small differences in the geometries of HEM molecules will affect calculated values of interaction energies in systems containing these HEM

molecules. This was confirmed in the recent study of the influence of hydrogen bonding on the electrostatic potential values of TNB, TNP, and TNT molecules [16]. To investigate the influence of small differences in the geometries of crystal structures on the energies of noncovalent interactions, model systems in which TNB geometries extracted from crystal structures were involved in C-H/O hydrogen bonds with the artificially added water molecule were used. TNP and TNT crystal structures were not used for the study of the influence of small differences in geometries on energies of hydrogen bonds since for these structures neutron diffraction data were not available for comparison. C-H/O interactions were chosen since visual inspection of extracted crystal structures showed that this type of interaction is very frequent in crystal structures of TNB, TNP, and TNT molecules (Figure S6) For all geometries based on X-ray data, hydrogen atom positions were normalized. Geometries in which the strongest C-H/O interactions in the TNB/H₂O system were calculated are given in Figure 7.

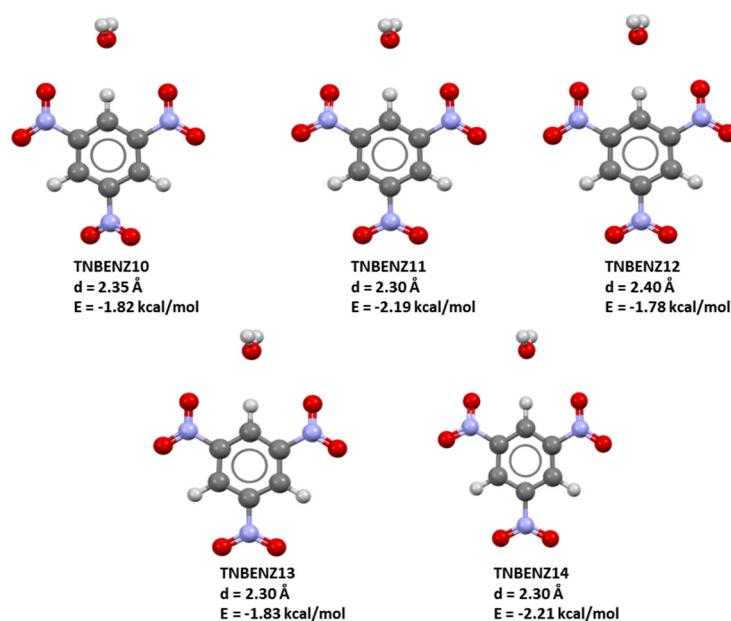


Figure 7. TNB/H₂O model systems containing TNB geometries extracted from crystal structures and artificially added water molecules. Calculated energies of the strongest interactions with corresponding O...H distances were given below every model system.

Results of interaction energy calculations showed that in all model systems calculated O...H distances were in the interval 2.30–2.40 Å, with corresponding interaction energies from −1.78 to −2.21 kcal/mol. This is in good agreement with previously obtained results for model system TNB/H₂O in which computationally optimized geometry of TNB molecule was used and in which O...H distance was calculated to be 2.35 Å, with the interaction energy $\Delta E = -1.76$ kcal/mol [16]. In the case of the model system containing TNBENZ10 crystal structure (which was determined by neutron diffraction) the same O...H distance was calculated (2.35 Å). In addition, the calculated interaction energy for this model system was in good agreement with the previously calculated interaction energy for the model system containing theoretically optimized geometry of TNB ($\Delta E = -1.82$ kcal/mol). In the case of the model system containing TNB geometry from crystal structure TNBENZ12, very similar interaction energy was calculated compared to the interaction energy obtained for the model system containing theoretically optimized geometry of TNB ($\Delta E = -1.78$ kcal/mol). However, in the case of model systems involving TNBENZ11 and TNBENZ14 geometries, significant differences in interaction energies were observed. For the model system TNBENZ14/H₂O calculated interaction energy was $\Delta E = -2.21$ kcal/mol which corresponds to a deviation of 17.65% compared to interaction energy calculated for the model system containing crystal structure determined using

neutron diffraction data. On the other hand, the deviation between interaction energies in model systems containing TNBENZ10 geometry and computationally optimized geometry was calculated to be only 3.30%.

4. Discussion

Results of electrostatic potential maps calculations showed that small differences in the geometries of crystal structures lead to significant differences in electrostatic potential values in the critical points located in the centers of TNB, TNP, and TNT molecules. In the case of the TNB molecule, the TNBEZN10 structure obtained by a very accurate neutron diffraction technique was available and used as reference geometry for further analysis. In the case of TNBENZ10 crystal structure, a value of positive potential above the central area of the molecular surface was calculated to be 27.42 kcal/mol. This was very close to the value previously obtained for the computationally optimized geometry (27.33 kcal/mol—0.35% deviation). However, for all other geometries extracted from crystal structures calculated values of electrostatic potentials in selected critical points were significantly larger (30.26–30.76 kcal/mol) and deviations were in the interval of 10–13%. This deviation is larger than the deviation in electrostatic potential values between different molecules of explosive. For example, the value of electrostatic potential in the center of a computationally optimized TNP molecule is 27.49 kcal/mol which is a deviation of only 0.58% compared to the value calculated for the TNB molecule (27.33 kcal/mol) [16]. This can lead to serious consequences since values of electrostatic potentials are routinely used to predict the impact sensitivities of high-energy molecules.

Since the value of electrostatic potentials calculated for computationally optimized geometry of TNB was in good agreement with the value calculated for geometry obtained by neutron diffraction experiment, we used computationally optimized geometries as a reference for other two structures for which neutron diffraction data were not available.

In the case of the TNP molecule, calculated deviations from electrostatic potential values obtained for computationally optimized geometry were in the interval 7.56–19.40%. This represents a large discrepancy even in the case of the PICRAC structure for which a 7.56% deviation ($V_{\max} = 29.57$ kcal/mol) was calculated. It is important to note that for all other crystal structures deviations in electrostatic potential values compared to computationally optimized geometry were in the interval 13.86–19.40% which is quite large.

A somewhat better agreement was achieved when comparing electrostatic potentials calculated for geometries of TNT molecules extracted from crystal structures with results obtained for computationally optimized geometries. In the case of the ZZZMUC06 geometry, an excellent agreement between the electrostatic potential in critical points was achieved compared to the results obtained for the computationally optimized geometry (calculated deviation was 0.00%). However, in the cases of ZZZMUC01 and ZZZMUC05 quite large deviations were calculated (7.98 and 5.20%, respectively).

Significant differences in the values of electrostatic potentials were detected for MEPs calculated using optimized TATB geometry and geometries extracted from crystal structures (21.01% for TATNBZ and 24.07% for TATNBZ03 crystal structures). Somewhat smaller, but still large differences were noticed in the case of optimized TETRYL geometry and geometries extracted from MTNANL and MTNANL01 crystal structures (12.93% for MTNANL and 13.09% for MTANL01 crystal structures).

Electrostatic potential values on the molecular surfaces will be different for the nitroaromatic molecules in the crystals and for free nitroaromatic molecules. Also, the MEP for the molecule in a crystal and the free molecule will have different gauge choices. For the free molecule, the MEP is equal to zero on the infinity, while in a crystal it is not equal to zero. In the study performed by Gadre and co-authors electrostatic potential maps were calculated for free ibuprofen molecule, ibuprofen dimer and two clusters of ibuprofen molecules [28]. Results showed that there were significant differences in the values of the electrostatic potentials between free ibuprofen molecule and ibuprofen molecules in clusters. In our study we extracted geometries of the studied molecules from the crystal

structures and calculated electrostatic potential maps for the structure without surrounding that is present in cluster. Overall, in the case of all five nitroaromatic molecules, for most of the crystal structures, significant deviations in electrostatic potential values in selected critical points were identified compared to the results obtained for the computationally optimized geometries. This raises some important questions related to the selection of the starting geometries for calculations of electrostatic potentials in the central regions of nitroaromatic molecules. Obviously, the best choice would be geometry extracted from the crystal structure which was determined by a neutron diffraction experiment. However, if that geometry is not available, our results for the TNB molecule indicate that electrostatic potential values obtained for computationally optimized geometries are much more reliable than values obtained using geometries extracted from crystal structures determined by X-ray experiments.

The focus of our study was on the values of the electrostatic potential in the critical points above the central regions of nitroaromatic molecules since these values are good indicators of the sensitivity of nitroaromatic molecules towards detonation. However, these small differences in geometries may affect electrostatic potential values in other parts of the molecular surface, too. This also indicates that differences in geometries may affect other important properties of nitroaromatic molecules like noncovalent bonding. One of the most common types of hydrogen bonds involving nitroaromatic molecules is the C-H/O interaction. Although there were no critical points located on the hydrogen atom along the extension of the C-H bond of studied nitroaromatic molecules, we compared C-H/O interaction energies calculated for different crystal structures of TNB molecules to study the influence of small differences in geometries on C-H/O interaction energies. TNB molecule was chosen since only for this molecule neutron diffraction structure was available, which was needed as a reference. Results of interaction energy calculations showed that O \cdots H distances were reasonably good in all model systems, however, interaction energy values varied from -1.78 to -2.21 kcal/mol. Compared to interaction energy calculated in the model system containing computationally optimized geometry ($\Delta E = -1.76$ kcal/mol) [16] this is a deviation of up to 17.56%, which is not negligible.

We have to point out that further studies of the influence of small differences in geometries of crystal structures on the values of electrostatic potential will be needed. The aim of this study was not to provide a detailed study of this phenomenon in a very general context but to raise awareness of the importance of the careful selection of input data for electrostatic potential maps calculations in the very particular case of nitroaromatic explosives since electrostatic potential values are used in practice for prediction of important properties of these explosives. However, the differences in geometries and energies of hydrogen bonds involving different crystal structures of the same molecule of TNB indicate that this problem can have much broader implications, especially in the fields of material science, noncovalent interactions, and host-guest systems.

Supplementary Materials: The following supporting information can be downloaded at: <https://www.mdpi.com/article/10.3390/cryst12101455/s1>, Figure S1: IR spectra calculated for the optimized TNB structure using M06/cc-PVDZ level of theory; Figure S2: IR spectra calculated for the optimized TNP structure using M06/cc-PVDZ level of theory; Figure S3: IR spectra calculated for the optimized TNT structure using M06/cc-PVDZ level of theory; Figure S4: IR spectra calculated for the optimized TATB structure using M06/cc-PVDZ level of theory; Figure S5: IR spectra calculated for the optimized TETRYL structure using M06/cc-PVDZ level of theory; Figure S6: C-H/O interactions between TNB molecules in the crystal structure TNBENZ10. The distance between interacting H and O atoms in this interaction is 2.25 Å, while C-H-O angle is 168.26°; Table S1: Crystal structures extracted from Cambridge structural Database containing TNB molecule; Table S2: Crystal structures extracted from Cambridge structural Database containing TNP molecule; Table S3: Crystal structures extracted from Cambridge structural Database containing TNT molecule.

Author Contributions: Conceptualization, D.Ž.V.; methodology, D.Ž.V.; validation, D.S.K. and V.B.M.; formal analysis, D.S.K. and V.B.M.; investigation, D.S.K.; resources, D.Ž.V.; data curation, D.Ž.V. and V.B.M.; writing—original draft preparation, D.Ž.V.; writing—review and editing, D.Ž.V.,

D.S.K. and V.B.M.; visualization, D.S.K.; supervision, D.Ž.V.; project administration, D.Ž.V.; funding acquisition, D.Ž.V. All authors have read and agreed to the published version of the manuscript.

Funding: This research was supported by the Science Fund of the Republic of Serbia, PROMIS, #6066886, CD-HEM. This work was supported by the Ministry of Education, Science and Technological Development of Republic of Serbia (Contract number: 451-03-68/2022-14/200168).

Data Availability Statement: Not applicable.

Conflicts of Interest: The authors declare no conflict of interest.

References

1. Liu, G.; Wei, S.-H.; Zhang, C. Review of the Intermolecular Interactions in Energetic Molecular Cocrystals. *Cryst. Growth Des.* **2020**, *20*, 7065–7079. [[CrossRef](#)]
2. Politzer, P.; Murray, J.S. Perspectives on the crystal densities and packing coefficients of explosive compounds. *Struct. Chem.* **2016**, *27*, 401–408. [[CrossRef](#)]
3. Born, M.; Plank, J.; Klapötke, T.M. Energetic Polymers: A Chance for Lightweight Reactive Structure Materials? *Prop. Explos. Pyrotech.* **2022**, *47*, e202100368. [[CrossRef](#)]
4. Politzer, P.; Murray, J.S. Some molecular/crystalline factors that affect the sensitivities of energetic materials: Molecular surface electrostatic potentials, lattice free space and maximum heat of detonation per unit volume. *J. Mol. Model.* **2015**, *21*, 25. [[CrossRef](#)]
5. Born, M.; Karaghiosoff, K.; Klapötke, T.M.; Voggenreiter, M. Oxetane Monomers Based On the Powerful Explosive LLM-116: Improved Performance, Insensitivity, and Thermostability. *ChemPlusChem* **2022**, *87*, e202200049. [[CrossRef](#)] [[PubMed](#)]
6. Nešić, J.; Cvijetić, I.N.; Bogdanov, J.; Marinković, A. Synthesis and Characterization of Azido Esters as Green Energetic Plasticizers. *Prop. Explos. Pyrotech.* **2021**, *46*, 1537–1546. [[CrossRef](#)]
7. Murray, J.S.; Concha, M.C.; Politzer, P. Links between surface electrostatic potentials of energetic molecules, impact sensitivities and C–NO₂/N–NO₂ bond dissociation energies. *Mol. Phys.* **2009**, *107*, 89–97.
8. Politzer, P.; Murray, J.S. High Performance, Low Sensitivity: Conflicting or Compatible? *Propellants Explos. Pyrotech.* **2016**, *41*, 414–425. [[CrossRef](#)]
9. Politzer, P.; Lane, P.; Murray, J.S. Electrostatic Potentials, Intralattice Attractive Forces and Crystal Densities of Nitrogen-Rich C,H,N,O Salts. *Crystals* **2016**, *6*, 7. [[CrossRef](#)]
10. Hammerl, A.; Klapötke, T.M.; Mayer, P.; Weigand, J.J. Synthesis, Structure, Molecular Orbital Calculations and Decomposition Mechanism for Tetrazolylazide CHN₇, its Phenyl Derivative PhCN₇ and Tetrazolylpentazole CHN₉. *Prop. Explos. Pyrotech.* **2005**, *30*, 17–26. [[CrossRef](#)]
11. Klapötke, T.M.; Nordheider, A.; Stierstorfer, J. Synthesis and reactivity of an unexpected highly sensitive 1-carboxymethyl-3-diazonio-5-nitrimino-1,2,4-triazole. *New J. Chem.* **2012**, *36*, 1463–1468. [[CrossRef](#)]
12. Politzer, P.; Lane, P.; Murray, J.S. Tricyclic polyazine n-oxides as proposed energetic compounds. *Cent. Eur. J. Energetic Mater.* **2013**, *10*, 305.
13. Krishnapriya, V.U.; Suresh, C.H. The use of electrostatic potential at nuclei in the analysis of halogen bonding. *New J. Chem.* **2022**, *46*, 6158–6164. [[CrossRef](#)]
14. Kim, C.K.; Cho, S.G.; Kim, C.K.; Park, H.-Y.; Zhang, H.; Lee, H.W. Prediction of densities for solid energetic molecules with molecular surface electrostatic potentials. *J. Comput. Chem.* **2008**, *29*, 1818–1824. [[CrossRef](#)]
15. Liu, Y.; Cao, Y.; Lai, W.; Yu, T.; Ma, Y.; Ge, Z. A strategy for predicting the crystal structure of energetic N-oxides based on molecular similarity and electrostatic matching. *CrystEngComm* **2021**, *23*, 714–723. [[CrossRef](#)]
16. Kretić, D.S.; Radovanović, J.I.; Veljković, D.Ž. Can the sensitivity of energetic materials be tuned by using hydrogen bonds? Another look at the role of hydrogen bonding in the design of high energetic compounds. *Phys. Chem. Chem. Phys.* **2021**, *23*, 7472–7479. [[CrossRef](#)] [[PubMed](#)]
17. Đunović, A.B.; Veljković, D.Ž. Halogen bonds as a tool in the design of high energetic materials: Evidence from crystal structures and quantum chemical calculations. *CrystEngComm* **2021**, *23*, 6915–6922. [[CrossRef](#)]
18. Eckhardt, C.J.; Gavezzotti, A. Computer Simulations and Analysis of Structural and Energetic Features of Some Crystalline Energetic Materials. *J. Phys. Chem. B* **2007**, *111*, 3430–3437. [[CrossRef](#)]
19. Aina, A.A.; Misquitta, A.J.; Phipps, M.J.S.; Price, S.L. Charge Distributions of Nitro Groups Within Organic Explosive Crystals: Effects on Sensitivity and Modeling. *ACS Omega* **2019**, *4*, 8614–8625. [[CrossRef](#)]
20. Hauf, C.; Salvador, A.-A.H.; Holtz, M.; Woerner, M.; Elsaesser, T. Phonon driven charge dynamics in polycrystalline acetylsalicylic acid mapped by ultrafast x-ray diffraction. *Struct. Dyn.* **2019**, *6*, 014503. [[CrossRef](#)]
21. Li, H.; Shu, Y.; Gao, S.; Chen, L.; Ma, Q.; Ju, X. Easy methods to study the smart energetic TNT/CL-20 co-crystal. *J. Mol. Model.* **2013**, *19*, 4909–4917. [[CrossRef](#)] [[PubMed](#)]
22. Groom, C.R.; Bruno, I.J.; Lightfoot, M.P.; Ward, S.C. The Cambridge Structural Database. *Acta Crystallogr. Sect. B Struct. Sci. Cryst. Eng. Mater.* **2016**, *B72*, 171–179. [[CrossRef](#)] [[PubMed](#)]
23. Frisch, M.J.; Trucks, G.W.; Schlegel, H.B.; Scuseria, G.E.; Robb, M.A.; Cheeseman, J.R.; Scalmani, G.; Barone, V.; Petersson, G.A.; Nakatsuji, H.; et al. *Gaussian 09, Revision A.02*; Gaussian, Inc.: Wallingford, CT, USA, 2016.

24. Bulat, F.A.; Toro-Labbe, A.; Brinck, T.; Murray, J.S.; Politzer, P. Quantitative analysis of molecular surfaces: Areas, volumes, electrostatic potentials and average local ionization energies. *J. Mol. Model.* **2010**, *16*, 1679–1691. [[CrossRef](#)] [[PubMed](#)]
25. Kretić, D.S.; Veljković, I.S.; Đunović, A.B.; Veljković, D.Ž. Chelate Coordination Compounds as a New Class of High-Energy Materials: The Case of Nitro-Bis(Acetylacetonato) Complexes. *Molecules* **2021**, *26*, 5438. [[CrossRef](#)] [[PubMed](#)]
26. Veljković, D.Ž.; Janjić, G.V.; Zarić, S.D. Are C–H•••O interactions linear? Case of aromatic CH donors. *CrystEngComm* **2011**, *13*, 5005–5010.
27. Macrae, C.F.; Sovago, I.; Cottrell, S.J.; Galek, P.T.A.; McCabe, P.; Pidcock, E.; Platings, M.; Shields, G.P.; Stevens, J.S.; Towler, M.; et al. Mercury 4.0: From visualization to analysis, design and prediction. *J. Appl. Cryst.* **2020**, *53*, 226–235. [[CrossRef](#)]
28. Babu, K.; Ganesh, V.; Gadre, S.; Ghermani, N.E. Tailoring approach for exploring electron densities and electrostatic potentials of molecular crystals. *Theor. Chem. Acc.* **2004**, *111*, 255–263. [[CrossRef](#)]